Design of Signal-Adapted Biorthogonal Filter Banks

Wu-Sheng Lu, *Senior Member, IEEE*, and Andreas Antoniou, *Fellow, IEEE*

***Abstract*—A method for the design of signal-adapted, M-channel biorthogonal filter banks of finite length is presented. The design problem is formulated as a constrained optimization problem and is solved by converting it into an iterative line-search problem through a first-order parameterization of the perfect reconstruction constraint. It is also shown for the two-channel case that if the analysis and synthesis lowpass filters are of different lengths, a refinement of the algorithm is possible that leads to a solution in a very small neighborhood of a local minimizer, which satisfies the perfect reconstruction (PR) constraint precisely.**

***Index Terms*—Biorthogonal filter banks, coding-gain maximization, constrained optimization, signal-adapted filter banks.**

I. Introduction

DURING the past several years, there has been a great deal of interest in the design of optimal orthogonal and biorthogonal filter banks in terms of some coding gain criterion [1]–[11]. Biorthogonal filter banks can offer improved performance over orthogonal filter banks [12], [13], but the optimal design of an M-channel biorthogonal filter bank requires the solution of a sophisticated constrained minimization problem [11].

In this paper, the design of signal-adapted, M-channel, biorthogonal filter banks of finite length is considered as a constrained optimization problem that attempts to minimize a coding gain related objective function [7], [11] subject to the perfect reconstruction condition. The basic approach to solve this problem is to first parameterize a first-order approximation of the perfect reconstruction (PR) constraint and then convert the constrained problem into an iterative line-search problem. In each iteration, the line search is carried out along a direction within the null space of a matrix characterized by the approximated PR condition. Closed-form formulas for the gradient vector and Hessian matrix of the objective function are derived to facilitate the identification of a good search direction such as a quasi-Newton or modified Newton direction. It is also shown for the two-channel case that if the analysis and synthesis lowpass filters are of different lengths, a refinement of the algorithm is possible that leads to a solution in a very small neighborhood of a local minimizer, which satisfies the PR constraint precisely. Simulation results are presented to illustrate the proposed design methods.

Manuscript received December 1, 1999; revised June 13, 2000. This paper was recommended by Associate Editor P. P. Vaidynathan. This work was supported by Micronet and the Natural Science and Engineering Research Council of Canada.

The authors are with the Department of Electrical and Computer Engineering, University of Victoria, Victoria, BC V8W 3P6, Canada (e-mail: wslu@ece.uvic.ca; andreas@ece.uvic.ca).

Publisher Item Identifier S 1057-7122(01)00648-1.

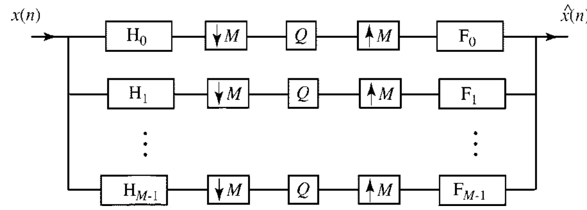

Fig. 1. M-channel maximally decimated uniform filter bank.

II. Problem Formulation

A. M-Channel Filter Banks and Perfect Reconstruction Condition

We consider the class of M-channel maximally decimated uniform filter banks where filters H_i and F_i for $0 \le i \le M-1$ are finite-duration impulse response (FIR) filters represented by transfer functions $H_i(z)$ and $F_i(z)$, respectively. Fig. 1 illustrates such a subband system, where the input signal $x(n)$ is assumed to be wide-sense stationary (WSS) [14] with a power spectral density $S_{xx}(\omega)$ and variance σ_x^2, and each of the blocks labeled with a $\mathcal{Q}$ represents a quantizer.

An M-channel filter bank is said to have the PR property if signal $\hat{x}(n)$ is a delayed version of the input signal $x(n)$ when the quantizers are replaced by direct paths. It is known [15] that an M-channel filter bank has the PR property if and only if the transfer functions $H_i(z)$ and $F_i(z)$ for $0 \le i \le M-1$ are constrained to satisfy the conditions

$$T_0(z) = z^{-l} \tag{1a}$$
$$T_k(z) = 0 \qquad \text{for } 1 \le k \le M-1 \tag{1b}$$

where

$$T_k(z) = \frac{1}{M}\sum_{i=o}^{M-1} F_i(z)H_i(W^k z)$$
$$W = e^{-j2\pi/M} \tag{1c}$$

Parameter l in (1a) is an integer that depends on the lengths of the FIR filters used. In the sequel, the above conditions are referred to collectively as the PR condition and an M-channel filter bank satisfying these conditions is called a *biorthogonal filter bank*. Note that we are assuming a normalized sampling period $T = 1$ s throughout the paper, i.e., the Nyquist frequency is deemed to be π rad/s.

B. Design Based on Coding Gain Criterion

Assume that the quantizer $\mathcal{Q}$ in the ith channel takes an arbitrary real number and converts it into a b_i-bit fraction using some arithmetic rule. We also assume optimal bit allocation with fixed bit rate $b = \sum_{i=0}^{M-1} b_i$. It has been shown in [11] that the mean-square reconstruction error is given by

$$E = cM2^{-2b}\Phi^{1/M} \tag{2}$$

where c is a constant and

$$\Phi = \prod_{i=0}^{M-1} \int_0^{2\pi} S_{xx}(e^{j\omega})|H_i(e^{j\omega})|^2 \frac{d\omega}{2\pi} \int_0^{2\pi} |F_i(e^{j\omega})|^2 \frac{d\omega}{2\pi} \tag{3}$$

with $H_i(e^{j\omega})$ and $F_i(e^{j\omega})$ being the frequency responses of filters H_i and F_i, respectively.

For a WSS input, the performance of the subband system can be measured in terms of the coding gain, $G_{SBC}(M)$, which is defined as the ratio of the mean-square value of the roundoff quantization error, E_{direct}, to the average variance of the reconstruction error in the subband system given by

$$E_{SBC} = \sum_{i=0}^{M-1} E[|\hat{x}(n) - x(n)|^2]/M$$

i.e.,

$$G_{SBC}(M) = \frac{E_{\text{direct}}}{E_{SBC}}. \tag{4}$$

As shown in [11], the coding gain can be expressed as

$$G_{SBC}(M) = \frac{\sigma_x^2}{\Phi^{1/M}}$$

where Φ is defined in (3).

In the next section, we develop a method for the design of M-channel biorthogonal filter banks that maximizes the coding gain by minimizing Φ in (3). The problem at hand is formulated in terms of the nonlinear constrained optimization problem

$$\text{minimize } \Phi \tag{5a}$$

$$\text{subject to the constraints in (1).} \tag{5b}$$

III. New Design Method

A. Objective Function Φ

Assume for the sake of simplicity that all the filters involved in the subband system have the same length N, and denote

$$H_i(z) = \sum_{k=0}^{N-1} h_{i,k} z^{-k} \qquad \text{for } 0 \le i \le M-1 \tag{6a}$$

$$F_i(z) = \sum_{k=0}^{N-1} f_{i,k} z^{-k} \qquad \text{for } 0 \le i \le M-1 \tag{6b}$$

and let

$$\boldsymbol{h}_i = [h_{i,0} \; \cdots \; h_{i,N-1}]^T \quad \text{and} \quad \boldsymbol{f}_i = [f_{i,0} \; \cdots \; f_{i,N-1}]^T$$

be the coefficient vectors of the filters. Function Φ in (3) can be expressed as

$$\Phi = \prod_{i=0}^{M-1} (\boldsymbol{h}_i^T \boldsymbol{R} \boldsymbol{h}_i) \prod_{i=0}^{M-1} ||\boldsymbol{f}_i||^2 \tag{7a}$$

where

$$\boldsymbol{R} = \int_0^{2\pi} S_{xx}(\omega) \cdot \begin{bmatrix} 1 & \cos\omega & \cdots & \cos[(N-1)\omega] \\ \cos\omega & 1 & & \\ \vdots & & \ddots & \\ \cos[(N-1)\omega] & & & 1 \end{bmatrix} \frac{d\omega}{2\pi}. \tag{7b}$$

Note that matrix $\boldsymbol{R}$ in (7b) is a symmetric positive definite Toeplitz matrix whose first column is $[r_0 \; r_1 \; \cdots \; r_{N-1}]^T$ where

$$r_k = \frac{1}{2\pi} \int_0^{2\pi} S_{xx}(e^{j\omega}) \cos k\omega \, d\omega. \tag{7c}$$

Now let

$$\boldsymbol{x} = [\boldsymbol{h}_0^T \;\; \cdots \;\; \boldsymbol{h}_{M-1}^T \;\; \boldsymbol{f}_0^T \;\; \cdots \;\; \boldsymbol{f}_{M-1}^T]^T \tag{8}$$

be the vector comprising all the coefficient vectors $\boldsymbol{h}_i$ and $\boldsymbol{f}_i$ for $0 \le i \le M-1$ and define

$$\alpha = \prod_{i=0}^{M-1} \boldsymbol{h}_i^T \boldsymbol{R} \boldsymbol{h}_i \tag{9a}$$

$$\alpha_k = \frac{\alpha}{\boldsymbol{h}_k^T \boldsymbol{R} \boldsymbol{h}_k} \tag{9b}$$

$$\alpha_{k,l} = \frac{\alpha}{(\boldsymbol{h}_k^T \boldsymbol{R} \boldsymbol{h}_k)(\boldsymbol{h}_l^T \boldsymbol{R} \boldsymbol{h}_l)} \tag{9c}$$

$$\beta = \prod_{i=0}^{M-1} ||\boldsymbol{f}_i||^2 \tag{10a}$$

$$\beta_k = \frac{\beta}{||\boldsymbol{f}_k||^2} \tag{10b}$$

$$\beta_{k,l} = \frac{\beta}{||\boldsymbol{f}_k||^2 ||\boldsymbol{f}_l||^2}. \tag{10c}$$

The gradient vector $\Phi(\boldsymbol{x})$ can be computed explicitly as

$$\nabla_x \Phi = \begin{bmatrix} \boldsymbol{g}_h \\ \boldsymbol{g}_f \end{bmatrix} \tag{11a}$$

where

$$\boldsymbol{g}_h = \begin{bmatrix} \boldsymbol{g}_{h_0} \\ \vdots \\ \boldsymbol{g}_{h_{M-1}} \end{bmatrix} \tag{11b}$$

with

$$\boldsymbol{g}_{h_k} = 2\alpha_k \beta \boldsymbol{R} \boldsymbol{h}_k \qquad \text{for } 0 \le k \le M-1$$

and

$$\boldsymbol{g}_f = \begin{bmatrix} \boldsymbol{g}_{f_0} \\ \vdots \\ \boldsymbol{g}_{f_{M-1}} \end{bmatrix} \tag{11c}$$

with

$$\boldsymbol{g}_{f_k} = 2\alpha\beta_k \boldsymbol{f}_k \qquad \text{for } 0 \le k \le M-1.$$

Similary, the Hessian matrix can be computed as

$$\nabla_{xx}^2 \Phi = \begin{bmatrix} \boldsymbol{H}_{hh} & \boldsymbol{H}_{hf} \\ \boldsymbol{H}_{hf}^T & \boldsymbol{H}_{ff} \end{bmatrix} \tag{12a}$$

where

$$\boldsymbol{H}_{hh} = \begin{bmatrix} \boldsymbol{H}_{0,0} & \cdots & \boldsymbol{H}_{0,M-1} \\ \vdots & & \vdots \\ \boldsymbol{H}_{M-1,0} & \cdots & \boldsymbol{H}_{M-1,M-1} \end{bmatrix} \tag{12b}$$

with

$$\boldsymbol{H}_{k,l} = \begin{cases} 2\alpha_k \beta \boldsymbol{R} & \text{for } l = k \\ 4\alpha_{kl}\beta \boldsymbol{R}\boldsymbol{h}_k\boldsymbol{h}_l^T\boldsymbol{R} & \text{for } l \neq k \end{cases}$$

$$\boldsymbol{H}_{hf} = \begin{bmatrix} \boldsymbol{G}_{0,0} & \cdots & \boldsymbol{G}_{0,M-1} \\ \vdots & & \vdots \\ \boldsymbol{G}_{M-1,0} & \cdots & \boldsymbol{G}_{M-1,M-1} \end{bmatrix} \tag{12c}$$

with

$$\boldsymbol{G}_{k,l} = 4\alpha_k\beta_l \boldsymbol{R}\boldsymbol{h}_k\boldsymbol{f}_l^T$$

and

$$\boldsymbol{H}_{ff} = \begin{bmatrix} \boldsymbol{F}_{0,0} & \cdots & \boldsymbol{F}_{0,M-1} \\ \vdots & & \vdots \\ \boldsymbol{F}_{M-1,0} & \cdots & \boldsymbol{F}_{M-1,M-1} \end{bmatrix} \tag{12d}$$

with

$$\boldsymbol{F}_{k,l} = \begin{cases} 2\alpha\beta_k \boldsymbol{I} & \text{for } k = l \\ 4\alpha\beta_{kl}\boldsymbol{f}_k\boldsymbol{f}_l^T & \text{for } k \neq l. \end{cases}$$

The dimension of parameter vector $\boldsymbol{x}$ in (8) is $2MN$. Since these parameters are constrained to satisfy the PR condition and possibly additional conditions (e.g., to achieve linear phase response, etc.), they are not independent of each other but are related to a reduced set of independent parameters. Accordingly, the minimization problem in (5) can be reduced in size but the gradient vector and Hessian matrix of Φ with respect to the new (and independent) parameter vector need to be evaluated. These computations can be carried out using $\nabla_x\Phi$ and $\nabla_{xx}^2\Phi$ in conjunction with the use of the Jacobian of vector $\boldsymbol{x}$ with respect to the new parameter vector as described in Section III-E.

B. Time-Domain PR Condition

The PR condition in (1) can be expressed in the time domain. Compared to its frequency-domain version, the PR condition in the time domain does not depend on the frequency parameter and can be made more explicit in terms of the filter coefficients. Consequently, it is more suitable in an optimization setting.

Let $\boldsymbol{P}$ and $\boldsymbol{Q}$ be the matrices that comprise the coefficients of the analysis filters and synthesis filters, respectively, i.e.,

$$\boldsymbol{P} = \begin{bmatrix} \boldsymbol{h}_0^T \\ \vdots \\ \boldsymbol{h}_{M-1}^T \end{bmatrix} \qquad \boldsymbol{Q} = \begin{bmatrix} \boldsymbol{f}_0^T \\ \vdots \\ \boldsymbol{f}_{M-1}^T \end{bmatrix}. \tag{13}$$

Without loss of generality, we assume that $N = ML$ for some integer L, and partition each of matrices $\boldsymbol{P}$ and $\boldsymbol{Q}$ into L blocks as

$$\boldsymbol{P} = [\boldsymbol{P}_0 \;\cdots\; \boldsymbol{P}_{L-1}] \qquad \boldsymbol{Q} = [\boldsymbol{Q}_0 \;\cdots\; \boldsymbol{Q}_{L-1}] \tag{14}$$

where each $\boldsymbol{P}_i$ and $\boldsymbol{Q}_i$ is an $M \times M$ matrix. The time-domain PR condition can then be expressed as [16]

$$\boldsymbol{A}(\boldsymbol{P})\tilde{\boldsymbol{Q}} = \boldsymbol{C} \tag{15}$$

where $\boldsymbol{A}(\boldsymbol{P})$ is the block Toeplitz matrix with $[\boldsymbol{P}_0^T \; \boldsymbol{0} \;\cdots\; \boldsymbol{0}] \in \mathbb{R}^{M\times LM}$ as its first row and $[\boldsymbol{P}_0 \; \boldsymbol{P}_1 \;\cdots\; \boldsymbol{P}_L \; \boldsymbol{0} \;\cdots\; \boldsymbol{0}]^T \in \mathbb{R}^{(2L-1)M\times M}$ as its first column, $\tilde{\boldsymbol{Q}} = [\boldsymbol{Q}_0^T \; \boldsymbol{Q}_1^T \;\cdots\; \boldsymbol{Q}_{L-1}^T]^T \in \mathbb{R}^{LM\times M}$, and $\boldsymbol{C} = [\boldsymbol{0} \;\cdots\; \boldsymbol{0} \; \boldsymbol{J} \; \boldsymbol{0} \;\cdots\; \boldsymbol{0}]^T \in \mathbb{R}^{(2L-1)M\times M}$ with

$$\boldsymbol{J} = \frac{\hat{\boldsymbol{I}}}{M} \qquad \text{with } \hat{\boldsymbol{I}} = \begin{bmatrix} \boldsymbol{0} & & 1 \\ & \iddots & \\ 1 & & \boldsymbol{0} \end{bmatrix}. \tag{16}$$

Alternatively, the PR condition can be expressed as

$$\boldsymbol{A}(\boldsymbol{Q})\tilde{\boldsymbol{P}} = \boldsymbol{C} \tag{17}$$

where $\boldsymbol{A}(\boldsymbol{Q})$ and $\tilde{\boldsymbol{P}}$ are obtained from $\boldsymbol{A}(\boldsymbol{P})$ and $\tilde{\boldsymbol{Q}}$ with blocks $\boldsymbol{P}_i$ and $\boldsymbol{Q}_i$ replaced by $\boldsymbol{Q}_i$ and $\boldsymbol{P}_i$, respectively.

For two given matrix sequences $\mathcal{P} = \{\boldsymbol{P}_0, \boldsymbol{P}_1, \ldots, \boldsymbol{P}_{L-1}\}$ and $\mathcal{Q} = \{\boldsymbol{Q}_0, \boldsymbol{Q}_1, \ldots, \boldsymbol{Q}_{L-1}\}$, we define the *matrix convolution* of $\mathcal{P}$ and $\mathcal{Q}$ as

$$\mathcal{S} = \text{conv}(\mathcal{P}, \mathcal{Q}) = \{\boldsymbol{S}_0, \ldots, \boldsymbol{S}_{2L-2}\} \tag{18}$$

where

$$\boldsymbol{S}_k = \sum_{i=0}^{L-1} \boldsymbol{P}_i^T \boldsymbol{Q}_{k-i} \qquad \text{for } 0 \leq k \leq 2L-2 \tag{19}$$

with the understanding that $\boldsymbol{P}_i$ and $\boldsymbol{Q}_i$ for $i < 0$ or $i > L-1$ are zero matrices. The matrix convolution is a natural extension of the discrete convolution of two scalar sequences, with which the time-domain PR condition can be simply stated as

$$\text{conv}(\mathcal{P}, \mathcal{Q}) = \mathcal{J} \tag{20}$$

where $\mathcal{J}$ is the impulse sequence defined by

$$\mathcal{J} = \{\boldsymbol{0}, \cdots, \boldsymbol{0}, \boldsymbol{J}, \boldsymbol{0}, \cdots, \boldsymbol{0}\} \tag{21}$$

with $\boldsymbol{J}$ defined in (16).

Note that, for matrix sequences, the convolutions $\text{conv}(\mathcal{P}, \mathcal{Q})$ and $\text{conv}(\mathcal{Q}, \mathcal{P})$ are not the same in general. However, an alternative PR condition can be obtained from (17) as

$$\text{conv}(\mathcal{Q}, \mathcal{P}) = \mathcal{J}. \tag{22}$$

By replacing the frequency-domain PR condition in (5b) by the time-domain PR condition given in (20) or (22), the optimization problem at hand can be formulated such that the variables appear in the constraints explicitly in a bilinear form. This bilinear representation is suitable for the subsequent first-order approximation of the PR condition and, for this reason, the time-domain PR condition will be used in the proposed method.

Given a nonoptimal initial design, which might not even satisfy the PR condition, the proposed design algorithm iteratively modifies the filter coefficients so as to better satisfy the PR condition and at the same time reduce the objective function Φ. This design approach is illustrated by the flow chart in Fig. 2.

C. Independent Design Variables

An additional constraint to the optimization problem at hand comes from the necessity of normalizing the filter coefficients.

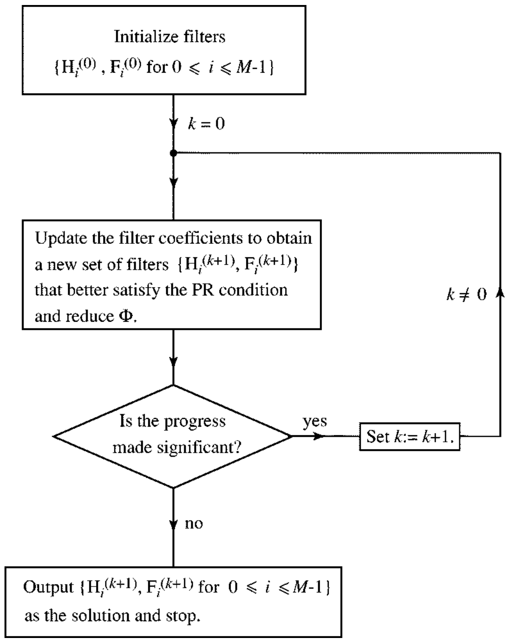

Fig. 2. Flowchart for the design of M-channel filter banks.

If all the analysis filters are rescaled by multiplying their coefficients by a nonzero scalar τ and at the same time all synthesis filters are rescaled by multiplying their coefficients by $1/\tau$, then the value of the objective function Φ remains the same. Under these circumstances, if the filter bank has the PR property and/or linear phase response, then so does the rescaled filter bank. Since this invariance holds for any τ, a solution may be obtained where the coefficients of $H_i(z)$ are very large and those of $F_i(z)$ are very small, or vice versa, and for such a solution numerical ill-conditioning could ensue. This problem can be prevented by imposing a constraint on the filter coefficients. A linear constraint of this type can be derived by requiring the sum of the filter gains at $\omega = 0$ to be a constant, e.g., we can impose the constraint

$$\sum_{i=0}^{M-1} \sum_{k=0}^{N-1} h_{i,k} = 1.$$

With this additional constraint incorporated, the problem formulation becomes

$$\text{minimize} \quad \Phi = \prod_{i=0}^{M-1} (\boldsymbol{h}_i^T \boldsymbol{R} \boldsymbol{h}_i) \|\boldsymbol{f}_i\|^2 \tag{23a}$$

$$\text{subject to:} \quad \text{conv}(\mathcal{P}, \mathcal{Q}) = \mathcal{J} \tag{23b}$$

$$\sum_{i=0}^{M-1} \sum_{k=0}^{N-1} h_{i,k} = 1. \tag{23c}$$

If the length of each of the filters H_i and F_i are assumed to be N for $0 \le i \le M-1$, then the total number of filter coefficients is $2MN$. The number of constraints in (23b) is equal to the number of entries in matrix $\boldsymbol{C}$ in (15), which is equal to $(2L-1)M^2 = 2MN - M^2$. This in conjunction with the constraint in (23c) gives the number of independent design parameters in (22) as $\eta = M^2 - 1$, which grows very rapidly with the number of channels M. It is interesting to note that η is *independent* of the length of the filters involved.

A technical difficulty in dealing with the constraint in (23b) is that the matrix convolution conv$(\mathcal{P}, \mathcal{Q})$ is bilinear with respect to the filter coefficients in $\mathcal{P}$ and $\mathcal{Q}$. Early methods handle this problem by fixing one of the filter banks so that (23b) becomes a set of linear constraints. However, by doing so, half of the filter coefficients cannot participate in the design and, consequently, the linearized constraints in (23b) become overdetermined [16]. In Section III-D, we shall develop a new linearization approach for (23b) by characterizing all acceptable changes in the filter coefficients surrounding a nominal M-channel filter bank such that the perturbed filter bank satisfies a first-order approximation of the PR condition.

An additional constraint, which is desirable in applications such as image compression, is that all filters H_i and F_i for $0 \le i \le M-1$ have linear phase response. If both the number of channels M and the filter length N are even, then a linear-phase analysis filter bank contains $M/2$ filters with symmetrical impulse responses and another $M/2$ filters with antisymmetrical impulse responses [17]. In such a case, the lower half of the equations in (15) are redundant and the time-domain PR condition reduces to

$$\begin{bmatrix} \boldsymbol{P}_0^T & \boldsymbol{0} & \cdots & \boldsymbol{0} \\ \boldsymbol{P}_1^T & \boldsymbol{P}_0^T & \cdots & \boldsymbol{0} \\ \vdots & \vdots & & \vdots \\ \boldsymbol{P}_{L-2}^T & \boldsymbol{P}_{L-3}^T & \cdots & \boldsymbol{0} \\ \tilde{\boldsymbol{I}}\boldsymbol{P}_{L-1}^T & \tilde{\boldsymbol{I}}\boldsymbol{P}_{L-2}^T & \cdots & \tilde{\boldsymbol{I}}\boldsymbol{P}_0^T \end{bmatrix} \begin{bmatrix} \boldsymbol{Q}_0 \\ \boldsymbol{Q}_1 \\ \vdots \\ \boldsymbol{Q}_{L-2} \\ \boldsymbol{Q}_{L-1} \end{bmatrix} = \begin{bmatrix} \boldsymbol{0} \\ \boldsymbol{0} \\ \vdots \\ \boldsymbol{0} \\ \tilde{\boldsymbol{I}}\boldsymbol{J} \end{bmatrix} \tag{24}$$

where $\tilde{\boldsymbol{I}} = [\boldsymbol{I}_{M/2}\ \boldsymbol{0}] \in R^{M/2 \times M}$, each of the first $M/2$ rows of $\boldsymbol{P}$ and $\boldsymbol{Q}$ defined in (14) is symmetric, and each of the last $M/2$ rows of $\boldsymbol{P}$ and $\boldsymbol{Q}$ is antisymmetric.

In (24), there are $(2L-1)M^2/2 = MN - M^2/2$ equations while the number of independent filter coefficients is MN. Thus there are $M^2/2 - 1$ independent parameters that can be used in the design. Again, the degrees of freedom for the design of M-channel linear-phase biorthogonal filter banks grows with the number of channels quickly but, as in the general case, it is independent of the filter length N. The optimization problem for the design of signal-adapted linear-phase M-channel biorthogonal filter banks can now be stated as

$$\text{minimize} \quad \Phi = \prod_{i=0}^{M-1} (\boldsymbol{h}_i^T \boldsymbol{R} \boldsymbol{h}_i) \|\boldsymbol{f}_i\|^2 \tag{25a}$$

$$\text{subject to:} \quad \text{Eqn. (24)} \tag{25b}$$

$$\sum_{i=0}^{M-1} \sum_{k=0}^{N/2-1} h_{i,k} = \frac{1}{2}. \tag{25c}$$

D. Parameterization of Design Variables

In this subsection we focus our attention on the general problem in (23). The objective function Φ in (23a) depends on vector $\boldsymbol{x}$ defined in (8). In the kth iteration of the optimization, point $\boldsymbol{x}_k$ is updated as

$$\boldsymbol{x}_{k+1} = \boldsymbol{x}_k + \Delta \boldsymbol{x} \tag{26}$$

where $\Delta \boldsymbol{x} = [\Delta \boldsymbol{h}_0^T \ \cdots \ \Delta \boldsymbol{h}_{M-1}^T \ \Delta \boldsymbol{f}_0^T \ \cdots \ \Delta \boldsymbol{f}_{M-1}^T]^T$ such that

1) if $\boldsymbol{x}_k$ does not satisfy the constraint in (23b), then $\boldsymbol{x}_{k+1}$ is a better approximate solution of the equations in (23b) than $\boldsymbol{x}_k$, and
2) $\Phi(\boldsymbol{x}_{k+1})$ is significantly smaller relative to $\Phi(\boldsymbol{x}_k)$.

Requirement 1) implies that the design will allow an initial point which corresponds to a filter bank that does not have the PR property, and if the algorithm converges, then the PR property will be satisfied at the limit point to within a prescribed tolerance. Requirement 2) assures that convergence will eventually be achieved.

Let $(\mathcal{P}_k, \mathcal{Q}_k)$ and $(\mathcal{P}_{k+1}, \mathcal{Q}_{k+1})$ be the matrix sequences $(\mathcal{P}, \mathcal{Q})$ associated with $\boldsymbol{x}_k$ and $\boldsymbol{x}_{k+1}$, respectively. It follows from (26) that these two sequences are related by

$$\mathcal{P}_{k+1} = \mathcal{P}_k + \Delta\mathcal{P} \tag{27a}$$
$$\mathcal{Q}_{k+1} = \mathcal{Q}_k + \Delta\mathcal{Q} \tag{27b}$$

where $\Delta\mathcal{P}$ and $\Delta\mathcal{Q}$ are two perturbation sequences that are *linearly* dependent on $\Delta\boldsymbol{x}$. The matrix convolution defined by (18) and (19) satisfies the equations

$$\begin{aligned}\operatorname{conv}(\alpha\mathcal{P}_1 + \beta\mathcal{P}_2, \mathcal{Q})\\ = \alpha\operatorname{conv}(\mathcal{P}_1, \mathcal{Q}) + \beta\operatorname{conv}(\mathcal{P}_2, \mathcal{Q})\end{aligned} \tag{28a}$$

and

$$\begin{aligned}\operatorname{conv}(\mathcal{P} + \alpha\mathcal{Q}_1 + \beta\mathcal{Q}_2)\\ = \alpha\operatorname{conv}(\mathcal{P}, \mathcal{Q}_1) + \beta\operatorname{conv}(\mathcal{P}, \mathcal{Q}_2)\end{aligned} \tag{28b}$$

where α and β are constants. Hence at the kth iteration, constraint (23b) becomes

$$\begin{aligned}\operatorname{conv}(\mathcal{P}_{k+1}, \mathcal{Q}_{k+1}) &= \operatorname{conv}(\mathcal{P}_k, \mathcal{Q}_k) + \operatorname{conv}(\Delta\mathcal{P}, \mathcal{Q}_k)\\ &\quad + \operatorname{conv}(\mathcal{P}_k, \Delta\mathcal{Q}) + \operatorname{conv}(\Delta\mathcal{P}, \Delta\mathcal{Q})\\ &= \mathcal{J}\end{aligned} \tag{29}$$

which leads to

$$\operatorname{conv}(\Delta\mathcal{P}, \mathcal{Q}_k) + \operatorname{conv}(\mathcal{P}_k, \Delta\mathcal{Q}) = \hat{\mathcal{J}} \tag{30}$$

where

$$\hat{\mathcal{J}} = \mathcal{J} - \operatorname{conv}(\mathcal{P}_k, \mathcal{Q}_k) - \operatorname{conv}(\Delta\mathcal{P}, \Delta\mathcal{Q}). \tag{31}$$

There are two ways to deal with the quadratic term $\operatorname{conv}(\Delta\mathcal{P}, \Delta\mathcal{Q})$ in (31). Suppose the design algorithm converges, then $\Delta\boldsymbol{x}$ in (26) approaches zero as $k \to \infty$. Since both $\Delta\mathcal{P}$ and $\Delta\mathcal{Q}$ are linearly related to $\Delta\boldsymbol{x}$, we have $\Delta\mathcal{P} \to 0$ and $\Delta\mathcal{Q} \to 0$ as $k \to \infty$. Hence $\operatorname{conv}(\Delta\mathcal{P}, \Delta\mathcal{Q})$ in (31) is a small quantity in terms of higher powers of the perturbation and can be neglected to linearize (30) with $\hat{\mathcal{J}} = \hat{\mathcal{J}}_0$ where

$$\hat{\mathcal{J}}_0 = \mathcal{J} - \operatorname{conv}(\mathcal{P}_k, \mathcal{Q}_k). \tag{32}$$

In addition, the constraint in (23c) at $\boldsymbol{x}_k + \Delta\boldsymbol{x}$ remains linear, i.e.,

$$\sum_{i=o}^{M-1}\sum_{k=0}^{N-1}(h_{i,k} + \Delta h_{i,k}) = 1.$$

Since (23c) is satisfied at $\boldsymbol{x}_k$, we have

$$\sum_{i=o}^{M-1}\sum_{k=0}^{N-1}\Delta h_{i,k} = 0$$

i.e.,

$$\boldsymbol{e}^T\Delta\boldsymbol{x} = 0 \tag{33}$$

where $\boldsymbol{e} = [1 \ \cdots \ 1 \ 0 \ \cdots \ 0]^T$ is the vector of dimension $2MN$ with the first half of its components equal unity and the remaining half equal to zero. The linearized equation (30) with $\hat{\mathcal{J}} = \mathcal{J}_0$ is now combined with (33) to form the complete set of linear constraints as

$$\boldsymbol{\Gamma}\Delta\boldsymbol{x} = \boldsymbol{\gamma}_0 \tag{34}$$

where $\boldsymbol{\Gamma} \in \mathbb{R}^{(2Mn-M^2+1)\times 2Mn}$ and $\boldsymbol{\gamma}_0 \in \mathbb{R}^{(2Mn-M^2+1)\times 1}$. For any $M > 1$, the linear system in (34) is underdetermined; consequently, all of its solutions can be parameterized as a linear function of an $(M^2 - 1)$-dimensional free parameter vector. This parameterization can conveniently be achieved by using the singular-value decomposition (SVD) of matrix $\boldsymbol{\Gamma}$ [18], i.e.,

$$\boldsymbol{\Gamma} = \boldsymbol{U}\boldsymbol{\Sigma}\boldsymbol{V}^T \tag{35}$$

where $\boldsymbol{U}$ and $\boldsymbol{V}$ are orthogonal matrices of sizes $2MN - M^2 + 1$ and $2MN$, respectively, and $\boldsymbol{\Sigma} = [\boldsymbol{\Sigma}_1 \ \ \boldsymbol{0}]$ with $\boldsymbol{\Sigma}_1 = \operatorname{diag}\{\sigma_1, \cdots, \sigma_{2Mn-M^2+1}\} \succ \boldsymbol{0}$, i.e., $\boldsymbol{\Sigma}_1$ is a positive definite matrix. All the solutions of (34) can be characterized as

$$\Delta\boldsymbol{x} = \boldsymbol{\delta}_0 + \boldsymbol{V}_\eta\boldsymbol{\xi} \tag{36}$$

where $\boldsymbol{\delta}_0 = \boldsymbol{\Gamma}^\dagger\boldsymbol{\gamma}_0$ with $\boldsymbol{\Gamma}^\dagger$ being the Moore–Penrose pseudo-inverse of $\boldsymbol{\Gamma}$, $\boldsymbol{V}_\eta$ consists of the last $\eta = M^2 - 1$ columns of $\boldsymbol{V}$, and $\boldsymbol{\xi} \in \mathbb{R}^{\eta\times 1}$ is an $(M^2 - 1)$-dimensional free parameter vector.

An alternative way to handle the nonlinearity in (31) is to use the increment matrix sequences $\Delta\mathcal{P}$ and $\Delta\mathcal{Q}$ obtained from the preceding iteration to evaluate the bilinear term $\operatorname{conv}(\Delta\mathcal{P}, \Delta\mathcal{Q})$. Denoting $\Delta\mathcal{P}$ and $\Delta\mathcal{Q}$ as $\hat{\Delta}\mathcal{P}$ and $\hat{\Delta}\mathcal{Q}$, respectively, (30) can be linearized with $\hat{\mathcal{J}} = \hat{\mathcal{J}}_1$ where

$$\hat{\mathcal{J}}_1 = \mathcal{J} - \operatorname{conv}(\mathcal{P}_k, \mathcal{Q}_k) - \operatorname{conv}(\hat{\Delta}\mathcal{P}, \hat{\Delta}\mathcal{Q}). \tag{37}$$

Accordingly, (34) is replaced by

$$\boldsymbol{\Gamma}\Delta\boldsymbol{x} = \boldsymbol{\gamma}_1 \tag{38}$$

where $\boldsymbol{\gamma}_1 \in \mathbb{R}^{(2Mn-M^2+1)\times 1}$ is determined by $\hat{\mathcal{J}}_1$ in (37) and all the solutions of (38) are characterized by

$$\Delta\boldsymbol{x} = \boldsymbol{\delta}_1 + \boldsymbol{V}_\eta\boldsymbol{\xi} \tag{39}$$

where $\boldsymbol{\delta}_1 = \boldsymbol{\Gamma}^\dagger\boldsymbol{\gamma}_1$.

E. Design Algorithm

The design of a signal-adapted M-channel biorthogonal filter bank is achieved by solving the constrained minimization problem in (23) in an iterative manner as described below.

1) Given the number of channels M and filter length N with $N = ML$ for some integer L, the algorithm starts with an

initial set of FIR filters $\{\mathrm{H}_i^{(0)},\, \mathrm{F}_i^{(0)},\, 0 \le i \le M-1\}$ that form an M-channel filter bank. Since (23) is a constrained nonlinear programming problem, a good initial point is preferred as it can affect the performance and efficiency of the algorithm in a positive way. A reasonable initial point that does not need to be optimum or to satisfy the PR condition can be obtained in a number of ways, for example, by using the method in [15]. Before going to the next step, we perform coefficient normalization to ensure that the constraint in (23c) holds for $\{h_{i,k}^{(0)},\, 0 \le i \le M-1,\, 0 \le k \le n-1\}$.

2) At the kth iteration, a point $\boldsymbol{x}_k$, which is associated with transfer functions $\{H_i^{(k)}(z),\, F_i^{(k)}(z),\, 0 \le i \le M-1\}$, is available. Point $\boldsymbol{x}_k$ is updated as

$$\boldsymbol{x}_{k+1} = \boldsymbol{x}_k + \Delta\boldsymbol{x} \tag{40}$$

where $\Delta\boldsymbol{x}$ is given by either (36) or (39) depending on whether $\hat{\mathcal{J}}$ in (30) is set to $\hat{\mathcal{J}} = \hat{\mathcal{J}}_0$ or $\hat{\mathcal{J}} = \hat{\mathcal{J}}_1$. In what follows, $\hat{\mathcal{J}} = \hat{\mathcal{J}}_0$ is assumed so that $\Delta\boldsymbol{x}$ is parameterized in terms of (36). The algorithm described below also holds for the case $\hat{\mathcal{J}} = \hat{\mathcal{J}}_1$.

Since $\boldsymbol{x}_k + \Delta\boldsymbol{x}$ with $\Delta\boldsymbol{x}$ given by (36) gives a first-order parameterization of the constraints in (23b) and (23c), at the kth iteration the problem in (23) is reduced to the *unconstrained* minimization problem

$$\underset{\boldsymbol{\xi} \in \mathbb{R}^\eta}{\text{minimize}}\; \Phi(\boldsymbol{x}_k + \boldsymbol{\delta}_0 + \boldsymbol{V}_\eta \boldsymbol{\xi}) \tag{41}$$

where $\boldsymbol{\xi}$ is the variable vector of dimension $\eta = M^2 - 1$. There are a number of robust and efficient algorithms available for unconstrained optimization [19]. These include the class of quasi-Newton methods, which require only the gradient vector $\nabla_\xi \Phi$, and the modified Newton method, which needs, in addition, the evaluation of the Hessian matrix $\nabla_{\xi\xi}\Phi$. The gradient vector and Hessian matrix of Φ with respect to variable $\boldsymbol{\xi}$ can be computed in closed form as

$$\nabla_\xi \Phi = \frac{\partial(\Delta\boldsymbol{x})}{\partial\boldsymbol{\xi}}\, \nabla_x \Phi(\boldsymbol{x})$$

and

$$\nabla_{\xi\xi}^2 \Phi = \frac{\partial(\Delta\boldsymbol{x})}{\partial\boldsymbol{\xi}}\, \nabla_{xx}^2 \Phi(\boldsymbol{x}) \left[\frac{\partial(\Delta\boldsymbol{x})}{\partial\boldsymbol{\xi}}\right]^T$$

where $\partial(\Delta\boldsymbol{x})/\partial\boldsymbol{\xi}$ denotes the Jacobian of $\Delta\boldsymbol{x}$ with respect to $\boldsymbol{\xi}$, which is given by $\boldsymbol{V}_\eta^T$ according to (36), $\nabla_x \Phi$ is given by (11), and $\nabla_{xx}^2 \Phi$ is given by (12). Thus, we have

$$\nabla_\xi \Phi = \boldsymbol{V}_\eta^T \nabla_x \Phi(\boldsymbol{x}) \tag{42}$$

$$\nabla_{\xi\xi}^2 \Phi = \boldsymbol{V}_\eta^T \nabla_{xx}^2 \Phi(\boldsymbol{x}) \boldsymbol{V}_\eta. \tag{43}$$

If $\boldsymbol{d}_k$ is a descent direction of $\Phi(\boldsymbol{x}_k + \boldsymbol{\delta}_0 + \boldsymbol{V}_\eta \boldsymbol{\xi})$ at $\boldsymbol{x}_k + \boldsymbol{\delta}_0$, then $\boldsymbol{\xi} = \alpha \boldsymbol{d}_k$ with $\alpha > 0$ reduces the value of objective function Φ. In a steepest-descent method (SDM), vector $\boldsymbol{d}_k$ is taken to be

$$\boldsymbol{d}_k = -\boldsymbol{g}_k \tag{44a}$$

where

$$\boldsymbol{g}_k = \boldsymbol{V}_\eta^T \nabla_x \Phi(\boldsymbol{x}_k + \boldsymbol{\delta}_0) \tag{44b}$$

while in the Broyden–Fletcher–Goldfarb–Shanno (BFGS) method

$$\boldsymbol{d}_k = -\boldsymbol{S}_k \boldsymbol{g}_k \tag{45a}$$

where $\boldsymbol{g}_k$ is given by (44b) and $\boldsymbol{S}_k$ is the positive-definite approximation of the inverse Hessian matrix. $\boldsymbol{S}_k$ is generated through the recursive relation

$$\boldsymbol{S}_{k+1} = \boldsymbol{S}_k + \left(1 + \frac{\boldsymbol{\gamma}_k^T \boldsymbol{S}_k \boldsymbol{\gamma}_k}{\boldsymbol{\gamma}_k^T \boldsymbol{\delta}_k}\right) \frac{\boldsymbol{\delta}_k \boldsymbol{\delta}_k^T}{\boldsymbol{\gamma}_k^T \boldsymbol{\delta}_k} - \frac{(\boldsymbol{\delta}_k \boldsymbol{\gamma}_k^T \boldsymbol{S}_k + \boldsymbol{S}_k \boldsymbol{\gamma}_k \boldsymbol{\delta}_k^T)}{\boldsymbol{\gamma}_k^T \boldsymbol{\delta}_k} \tag{45b}$$

where $\boldsymbol{S}_0 = \boldsymbol{I}$, $\boldsymbol{\delta}_k = \boldsymbol{x}_{k+1} - \boldsymbol{x}_k$, and $\boldsymbol{\gamma}_k = \boldsymbol{g}_{k+1} - \boldsymbol{g}_k$.

Once the search direction $\boldsymbol{d}_k$ is calculated, the optimum positive scalar α_k is determined by minimizing the function $\Phi(\boldsymbol{x}_k + \boldsymbol{\delta}_0 + \alpha \boldsymbol{V}_\eta + \boldsymbol{d}_k)$ with respect to α. This one-dimensional (1-D) minimization, often called a line search, can be performed efficiently if the gradient of the function is available [19]. In our case, however, the line search must be carried out in the vicinity of point $\boldsymbol{x}_k$ so that the vector increment $\Delta\boldsymbol{x}$ in (40) has a small magnitude and hence $\hat{\mathcal{J}}_0$ in (32) remains a good first-order approximation of $\hat{\mathcal{J}}$ in (31).

Suppose that the algorithm starts with an initial point at which the PR condition is at least approximately satisfied. Then $\boldsymbol{\delta}_0$ in (36) is small in magnitude. Further, notice that $||\boldsymbol{V}_\eta|| = 1$ and hence $||\alpha \boldsymbol{V}_\eta \boldsymbol{d}_k|| = \alpha ||\boldsymbol{d}_k||$. This suggests that point $\boldsymbol{x}_k$ should be updated as

$$\boldsymbol{x}_{k+1} = \boldsymbol{x}_k + \Delta^* \boldsymbol{x} \tag{46}$$

with

$$\Delta^* \boldsymbol{x} = \boldsymbol{\delta}_0 + \alpha_k \boldsymbol{V}_\eta \boldsymbol{d}_k \tag{47}$$

where $\boldsymbol{d}_k$ is given by (44) or (45) and is of length equal to unity, and α_k solves the 1-D minimization problem

$$\underset{\alpha}{\text{minimize}} \quad \Phi(\boldsymbol{x}_k + \boldsymbol{\delta}_0 + \alpha \boldsymbol{V}_\eta \boldsymbol{d}_k) \tag{48a}$$

$$\text{subject to} \quad 0 \le \alpha \le \alpha_{\max}. \tag{48b}$$

The upper bound $\alpha_{\max}$ in (48b) is selected to keep the norm of $\boldsymbol{\delta}_0 + \alpha \boldsymbol{V}_\eta^T \boldsymbol{d}_k$ small. With a normalized $\boldsymbol{d}_k$ and a reasonably small $\boldsymbol{\delta}_0$, an $\alpha_{\max}$ between 0.1 and 1.0 usually leads to satisfactory design results.

3) The two-norm of $\Delta^* \boldsymbol{x}$ is then used to check the progress made in the kth iteration in reducing $\Phi(\boldsymbol{x})$ as well as in satisfying the PR condition. If $||\Delta^* \boldsymbol{x}||$ is less than a prescribed tolerance ε, $\boldsymbol{x}_{k+1}$ is taken to be the solution $\boldsymbol{x}^*$ of the minimization problem and the algorithm is terminated. Otherwise, k is incremented to $k+1$ and the procedure is repeated from Step 2).

In effect, we have reduced the constrained optimization problem in (23), which contains $2MN$ design variables, to an iterative line-search problem on a small interval, as formulated

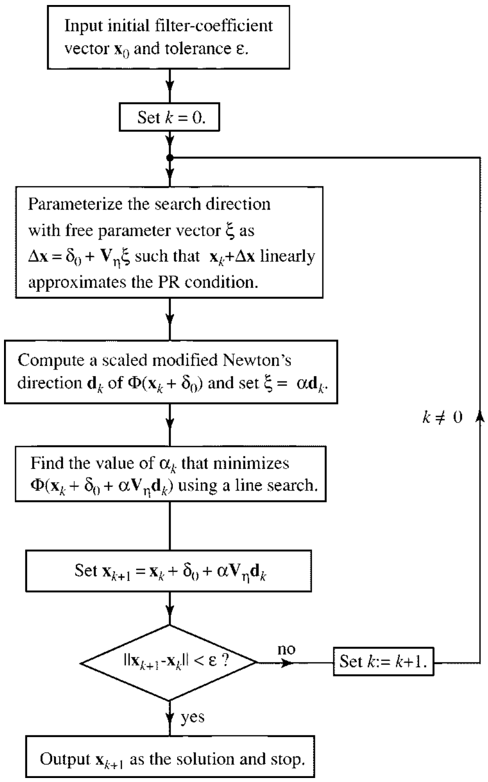

Fig. 3. Detailed flowchart for the design of M-channel filter banks.

in (48). At a solution point $\boldsymbol{x}^*$ of the problem in (48), the PR condition is approximately satisfied. This can be seen from (30) with $\hat{\mathcal{J}} = \mathcal{J}_0$, i.e.,

$$\text{conv}(\mathcal{P}_k,\, \mathcal{Q}_k)+\text{conv}(\Delta\mathcal{P},\, \mathcal{Q}_k)+\text{conv}(\mathcal{P}_k,\, \Delta\mathcal{Q}) = \mathcal{J}. \quad (49)$$

If the algorithm converges as $k \to \infty$, then $\Delta\mathcal{P}$ and $\Delta\mathcal{Q}$ approach the zero sequence; therefore, at the *theoretical* limit point $(\mathcal{P}^{**},\, \mathcal{Q}^{**})$, (49) becomes

$$\text{conv}(\mathcal{P}^{**},\, \mathcal{Q}^{**}) = \mathcal{J}.$$

As described in Step 3), however, our algorithm terminates as long as $||\Delta^*\boldsymbol{x}|| < \varepsilon$. This implies that a numerical solution $(\mathcal{P}^*,\, \mathcal{Q}^*)$ obtained from the algorithm can only satisfy the PR condition approximately, i.e.,

$$\text{conv}(\mathcal{P}^*,\, \mathcal{Q}^*) \approx \mathcal{J}. \quad (50)$$

However, since the degree to which the PR condition is satisfied depends on the termination tolerance ε, obviously, an *arbitrary precision can be achieved* by reducing the termination tolerance. The algorithm is illustrated by the flowchart of Fig. 3.

IV. Two-Channel Case

The two-channel case is of particular interest and will be further explored in this section for the following reasons. First, two-channel filter banks have been used extensively as building blocks in multirate digital signal processing systems with tree structures. Second, in the biorthogonal case, the lengths of the filters in the analysis filter bank can be different from those in the synthesis filter bank, as is often the case in subband image processing applications [20]–[22]. As will be shown here, the difference in filter lengths can be utilized to develop a two-stage design strategy for signal-adapted biorthogonal filter banks that satisfy the PR condition *precisely*.

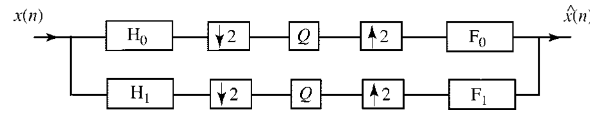

Fig. 4. Two-channel maximally decimated uniform filter bank.

A. Two-Channel Biorthogonal Linear-Phase Filter Bank

Throughout this section we consider the two-channel filter bank shown in Fig. 4 where H_0, F_0, H_1, and F_1 are linear-phase filters with transfer functions

$$\begin{aligned} H_0(z) &= z^{-N_1/2}\hat{H}_0(z), \\ \hat{H}_0(z) &= \sum_{i=-N_1/2}^{N_1/2} h_i z^{-i}, \qquad \text{with } h_i = h_{-i} \qquad (51a) \\ F_0(z) &= z^{-N_2/2}\hat{F}_0(z), \\ \hat{F}_0(z) &= \sum_{i=-N_2/2}^{N_2/2} f_i z^{-i}, \qquad \text{with } f_i = f_{-i} \\ H_1(z) &= F_0(-z) \\ F_1(z) &= -H_0(-z) \qquad (51b) \end{aligned}$$

where N_1, N_2 are even and $N_1 > N_2$. The above choice of $H_1(z)$ and $F_1(z)$ cancels the aliasing error and leads to the PR condition

$$H_0(z)F_0(z) - H_0(-z)F_0(-z) = 2z^{-(N_1+N_2)/2}. \quad (52)$$

From (52), it follows that the orders of filters H_0 and F_0, N_1 and N_2, respectively, must be chosen such that $(N_1+N_2)/2$ be an odd integer. Under these circumstances, (52) becomes

$$\hat{H}_0(z)\hat{F}_0(z) + \hat{H}_0(-z)\hat{F}_0(-z) = 2 \quad (53)$$

where $\hat{H}_0$ and $\hat{F}_0$ are zero-phase FIR filters whose transfer functions are defined in (51).

The objective function in (7) can now be written as

$$\Phi(\boldsymbol{x}) = (\boldsymbol{h}^T\boldsymbol{R}_1\boldsymbol{h})(\boldsymbol{f}^T\hat{\boldsymbol{R}}_2\boldsymbol{f})(\boldsymbol{h}^T\boldsymbol{Q}_1\boldsymbol{h})(\boldsymbol{f}^T\boldsymbol{Q}_2\boldsymbol{f}) \quad (54)$$

where $\boldsymbol{x} = [\boldsymbol{h}^T \;\; \boldsymbol{f}^T]^T$, $\boldsymbol{h} = [h_0 \;\; h_1 \;\; \cdots \;\; h_{N_1/2}]^T$, $\boldsymbol{f} = [f_0 \;\; f_1 \;\; \cdots \;\; f_{N_2/2}]^T$, and

$$\begin{aligned} \boldsymbol{R}_1 &= \frac{1}{2\pi}\int_0^{2\pi} S_{xx}(e^{j\omega})\boldsymbol{c}_{N_1}(\omega)\boldsymbol{c}_{N_1}^T(\omega)\,d\omega \\ \hat{\boldsymbol{R}}_2 &= \frac{1}{2\pi}\int_0^{2\pi} S_{xx}(e^{j\omega})\hat{\boldsymbol{c}}_{N_2}(\omega)\hat{\boldsymbol{c}}_{N_2}^T(\omega)\,d\omega \\ \boldsymbol{Q}_1 &= \text{diag}\{1,\, 2,\, \cdots,\, 2\} \in \mathbb{R}^{(1+(N_1/2))\times(1+(N_1/2))} \\ \boldsymbol{Q}_2 &= \text{diag}\{1,\, 2,\, \cdots,\, 2\} \in \mathbb{R}^{(1+(N_2/2))\times(1+(N_2/2))} \\ \boldsymbol{c}_{N_1}(\omega) &= \left[1 \; 2\cos\omega \; \cdots \; 2\cos\left[\frac{N_1}{2}\omega\right]\right]^T \\ \hat{\boldsymbol{c}}_{N_2}(\omega) &= \left[1 \; -2\cos\omega \; \cdots \; (-1)^{N_2/2}2\cos\left[\frac{N_2}{2}\omega\right]\right]^T. \end{aligned}$$

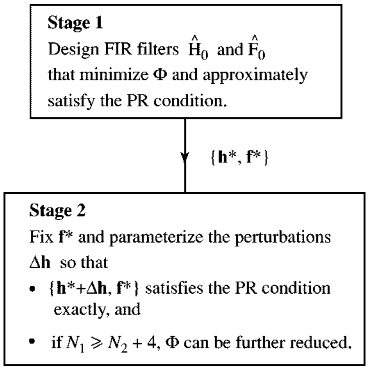

Fig. 5. Flowchart for the design of two-channel filter banks.

It can be verified that matrices $\boldsymbol{R}_1$ and $\hat{\boldsymbol{R}}_2$ in (54) are related to sequence $\{r_i,\, i = 0,\, 1,\, \cdots\}$ defined by (7c) as

$$\boldsymbol{R}_1 = \left[\hat{\boldsymbol{I}}_{N_1/2}\; \boldsymbol{I}_{1+(N_1/2)}\right] \boldsymbol{T}_{N_1} \begin{bmatrix} \hat{\boldsymbol{I}}_{N_1/2}^T \\ \boldsymbol{I}_{1+(N_1/2)} \end{bmatrix} \tag{55}$$

where $\boldsymbol{I}_{1+N_1/2}$ is the identity matrix of dimension $1 + N_1/2$,

$$\hat{\boldsymbol{I}}_{N_1/2} = \begin{bmatrix} 0 & \cdots & 0 \\ & & 1 \\ & \iddots & \\ 1 & & \end{bmatrix} \in \mathbb{R}^{(1+(N_1/2))\times(N_1/2)}, \tag{56}$$

and $\boldsymbol{T}_{N_1}$ is the symmetric Toeplitz matrix with $[r_0\; r_1\; \cdots\; r_{N_1}]$ as its first row, and

$$\hat{\boldsymbol{R}}_2 = \left[\hat{\boldsymbol{I}}_{N_2/2}\; \boldsymbol{I}_{1+(N_2/2)}\right] \hat{\boldsymbol{T}}_{N_2} \begin{bmatrix} \hat{\boldsymbol{I}}_{N_2/2}^T \\ \boldsymbol{I}_{1+(N_2/2)} \end{bmatrix} \tag{57}$$

where $\hat{\boldsymbol{T}}_{N_2}$ is the symmetric Toeplitz matrix with $[r_0\; -r_1\; \cdots\; (-1)^{N_2} r_{N_2}]$ as its first row.

The design problem at hand is to find transfer functions $\hat{H}_0(z)$ and $\hat{F}_0(z)$ that minimize $\Phi(\boldsymbol{x})$ in (54) subject to the PR condition in (53). In what follows, we develop a two-stage approach to obtain the design. The first stage is similar to that of Section III-D to generate a two-channel filter bank that satisfies a first-order approximation of the PR condition. The second stage takes advantage of the fact that $N_1 > N_2$ which allows, for a fixed $\boldsymbol{f}$, a parameterization of the perturbations of $\boldsymbol{h}$. This parameterization is then utilized in $\mathrm{H}_0(z)$ and $\mathrm{F}_0(z)$ to satisfy the PR condition in (52) exactly. If the length difference satisfies the inequality $N_1 - N_2 \geq 4$, then further reduction of the objective function Φ can also be achieved. The design method is illustrated by the flow chart in Fig. 5.

B. Design Stage 1

In the kth iteration, we update the coefficient vector $\boldsymbol{x}_k = [\boldsymbol{h}_k^T\; \boldsymbol{f}_k^T]^T$ as

$$\boldsymbol{x}_{k+1} = \boldsymbol{x}_k + \Delta\boldsymbol{x} \tag{58}$$

such that $\Phi(\boldsymbol{x}_{k+1})$ is less than $\Phi(\boldsymbol{x}_k)$ and $\boldsymbol{x}_{k+1}$ satisfies the PR condition in (53). In the first stage of the design, the increment vector $\Delta\boldsymbol{x}$ in (58) is parameterized so as to satisfy a first-order approximation of the PR condition, and the parameterized expression of $\boldsymbol{x}_{k+1}$ is then utilized to minimize the objective function $\Phi(\boldsymbol{x})$ defined in (54). This is done in a way similar to that of Section III-D. It can be shown that vector $\boldsymbol{x}_{k+1}$ in (58) satisfies a first-order approximation of the PR condition in (53) if the increment vector $\Delta\boldsymbol{x}$ satisfies the linear equation

$$[\boldsymbol{Q}_r\; \boldsymbol{P}_r]\Delta\boldsymbol{x} = -\boldsymbol{P}_r \boldsymbol{f}_k + \boldsymbol{e}_r \tag{59}$$

where $\boldsymbol{e}_r = [1\; 0\; \cdots\; 0]^T \in \mathbb{R}^{(N_1+N_2+2)/4\times 1}$, and matrices $\boldsymbol{P}_r \in \mathbb{R}^{(N_1+N_2+2)/4\times(N_2+2)/2}$, $\boldsymbol{Q}_r \in \mathbb{R}^{(N_1+N_2+2)/4\times(N_1+2)/2}$ are obtained as follows:

1) Generate Toeplitz matrix $\boldsymbol{Y}_0$ with $[h_{N_1/2}\; \cdots h_1\; h_0\; h_1\; \cdots\; h_{N_1/2}\; 0\; \cdots\; 0]^T \in \mathbb{R}^{(N_1+N_2+1)\times 1}$ as its first column and $[h_{N_1/2}\; 0\; \cdots\; 0] \in \mathbb{R}^{1\times(N_2+1)}$ as its first row.
2) Take the last $(N_1 + N_2)/2 + 1$ rows of $\boldsymbol{Y}_0$ to form matrix $\boldsymbol{Y}_1$.
3) Compute
$$\boldsymbol{Y}_2 = \boldsymbol{Y}_1 \begin{bmatrix} \hat{\boldsymbol{I}}_{N_2/2} \\ \boldsymbol{I}_{1+(N_2/2)} \end{bmatrix}.$$
4) Form matrix $\boldsymbol{P}_r$ by deleting the even numbered rows of $\boldsymbol{Y}_2$.
5) Similarly, form matrix $\boldsymbol{Q}_r$ with $[h_{N_1/2}\; \cdots h_1\; h_0\; h_1\; \cdots\; h_{N_1/2}\; 0\; \cdots\; 0]^T$ replaced by $[f_{N_2/2}\; \cdots\; f_1\; f_0\; f_1\; \cdots\; f_{N_2/2}\; 0\; \cdots\; 0]^T \in \mathbb{R}^{(N_1+N_2+1)\times 1}$ and $[h_{N_1/2}\; 0\; \cdots\; 0] \in \mathbb{R}^{1\times(N_2+1)}$ replaced by $[f_{N_2/2}\; 0\; \cdots\; 0] \in \mathbb{R}^{1\times(N_1+1)}$.

As for the general M-channel case discussed in Section III, it is necessary to add an additional constraint to normalize the filter coefficients. If the sum of the coefficients of $H_0(z)$ and $H_1(z)$ is required to be a constant, say, 1, the relation $H_1(z) = F_0(-z)$ and the linear phase-response constraint lead to

$$h_0 + 2\sum_{i=1}^{N_1/2} h_i + f_0 + 2\sum_{i=1}^{N_2/2} (-1)^i f_i = 1 \tag{60}$$

which further leads to a constraint on $\Delta\boldsymbol{x}$ as

$$\boldsymbol{e}_2^T \Delta\boldsymbol{x} = 0 \tag{61}$$

with $\boldsymbol{e}_2 = [1\; 2\; \cdots\; 2\; 1\; -2\; \cdots\; (-1)^{N_2/2}2]^T \in \mathbb{R}^{(((N_1+N_2)/2)+2)\times 1}$. Combining (59) and (61), the linear constraints on $\Delta\boldsymbol{x}$ can be expressed as

$$\boldsymbol{\Gamma}_2 \Delta\boldsymbol{x} = \boldsymbol{\gamma}_2 \tag{62}$$

where

$$\boldsymbol{\Gamma}_2 = \begin{bmatrix} \boldsymbol{Q}_r & \boldsymbol{P}_r \\ \hline \multicolumn{2}{c}{\boldsymbol{e}_2^T} \end{bmatrix}, \qquad \gamma_2 = \begin{bmatrix} -\boldsymbol{P}_r \boldsymbol{f}_k + \boldsymbol{e}_r \\ 0 \end{bmatrix}.$$

The total number of constraints in (62) is $(N_1 + N_2 + 6)/4$; hence the number of degrees of freedom contained in the $[(N_1 + N_2)/2 + 2]$-dimensional vector $\Delta\boldsymbol{x}$ is

$$\eta = \frac{N_1 + N_2 - 2}{4}. \tag{63}$$

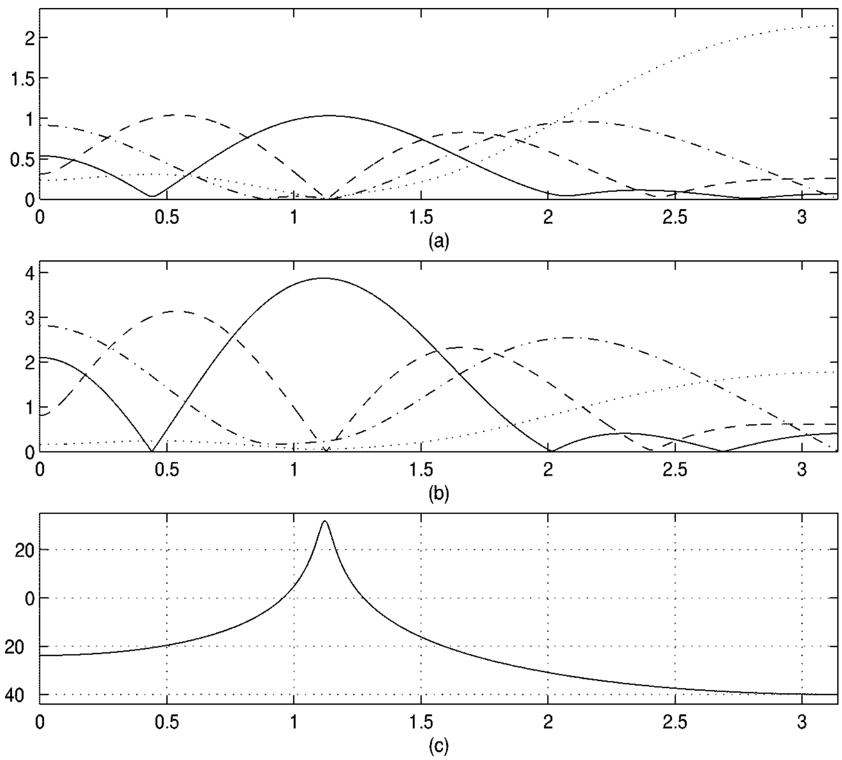

Fig. 6. Example A: (a) Amplitude responses of filters H_0 (solid line), H_1 (dashed line), H_2 (dash-dotted line), and H_3 (dotted line). (b) Amplitude responses of filters F_0 (solid line), F_1 (dashed line), F_2 (dash-dotted line), and F_3 (dotted line). (c) Power spectral density $S_{xx}(e^{j\omega})$ in decibels.

If the SVD of $\mathbf{\Gamma}_2$ is given by $\mathbf{\Gamma}_2 = \boldsymbol{U\Sigma V}^T$ and $\boldsymbol{V}_\eta$ is formed using the last η columns of $\boldsymbol{V}$, then all the solutions of (62) can be characterized by

$$\Delta \boldsymbol{x} = \boldsymbol{\delta}_2 + \boldsymbol{V}_\eta \boldsymbol{\xi} \tag{64}$$

where $\boldsymbol{\delta}_2 = \mathbf{\Gamma}_2^{\dagger}\boldsymbol{\gamma}_2$ and $\boldsymbol{\xi} \in \mathbb{R}^{\eta\times 1}$ is a free parameter vector. Now from (64) and (58), we have

$$\boldsymbol{x}_{k+1} = \boldsymbol{x}_k + \boldsymbol{\delta}_2 + \boldsymbol{V}_\eta \boldsymbol{\xi} \tag{65a}$$

with

$$\boldsymbol{\xi} = \alpha_k \boldsymbol{d}_k \tag{65b}$$

where $\boldsymbol{d}_k$ is a descent direction of $\Phi(\boldsymbol{x}_k + \boldsymbol{\delta}_2 + \boldsymbol{V}_\eta\boldsymbol{\xi})$ and α_k is a positive scalar that solves the line-search problem

$$\underset{\alpha}{\text{minimize}} \quad \Phi(\boldsymbol{x}_k + \boldsymbol{\delta}_2 + \alpha \boldsymbol{V}_\eta \boldsymbol{d}_k) \tag{66a}$$

$$\text{subject to} \quad 0 \le \alpha \le \alpha_{\max}. \tag{66b}$$

Typical choices of descent direction $\boldsymbol{d}_k$ include the steepest-descent direction

$$\boldsymbol{d}_k = -\boldsymbol{g}_k \tag{67a}$$

where

$$\boldsymbol{f}_k = \boldsymbol{V}_\eta^T \Phi_x(\boldsymbol{x}_k + \boldsymbol{\delta}_2) \tag{67b}$$

and the quasi-Newton direction

$$\boldsymbol{d}_k = -\boldsymbol{S}_k \boldsymbol{g}_k \tag{68}$$

where $\boldsymbol{S}_k$ is updated by using the BFGS formula given by (45b).

Having determined $\boldsymbol{\xi} = \boldsymbol{\alpha}_k \boldsymbol{d}_k$, the 2-norm of $\Delta\boldsymbol{x}$ in (64) is examined. If $||\Delta \boldsymbol{x}||$ is less than a prescribed tolerance ε, $\boldsymbol{x}_{k+1}$ is taken to be the solution $\boldsymbol{x}^*$ of the first stage of the design. Otherwise, with $k := k+1$, $\mathbf{\Gamma}_2$ and $\boldsymbol{\gamma}_2$ are updated using (62), $\boldsymbol{\delta}_2$ and $\boldsymbol{V}_\eta$ are recalculated using (64), and the 1-D minimization problem in (66) is solved to obtain a new $\Delta\boldsymbol{x}$.

C. Design Stage 2

The solution $\boldsymbol{x}^*$ obtained from design stage 1 satisfies the PR condition in (53) only *approximately*. As in the design method addressed in Section III, a solution $\boldsymbol{x}^*$ with improved approximation accuracy for the PR condition can be achieved by using a reduced tolerance ε at the cost of more iterations. As described below, an alternative approach for the solution of problem is possible by virtue of the fact that the lengths of filters H_0 and F_0 are different.

In a neighborhood of $\boldsymbol{x}^* = [\boldsymbol{h}^{*T} \;\; \boldsymbol{f}^{*T}]^T$, there are many points that satisfy the PR condition precisely. As a matter of fact, if we perturb $\boldsymbol{h}^*$ by $\Delta\boldsymbol{h}$ but keep $\boldsymbol{f}^*$ unaltered, then the first-order approximation of the PR condition in (59) becomes exact since the PR condition in (53) at point

$$\boldsymbol{x}^* + \Delta\boldsymbol{x} = \begin{bmatrix} \boldsymbol{h}^* + \Delta\boldsymbol{h} \\ \boldsymbol{f}^* \end{bmatrix} \tag{69}$$

contains no second or higher order terms. Therefore, in this case, (59) represents the PR condition exactly and can be written as

$$\boldsymbol{Q}_r^* \Delta\boldsymbol{h} = -\boldsymbol{P}_r^* \boldsymbol{f}^* + \boldsymbol{e}_r \tag{70}$$

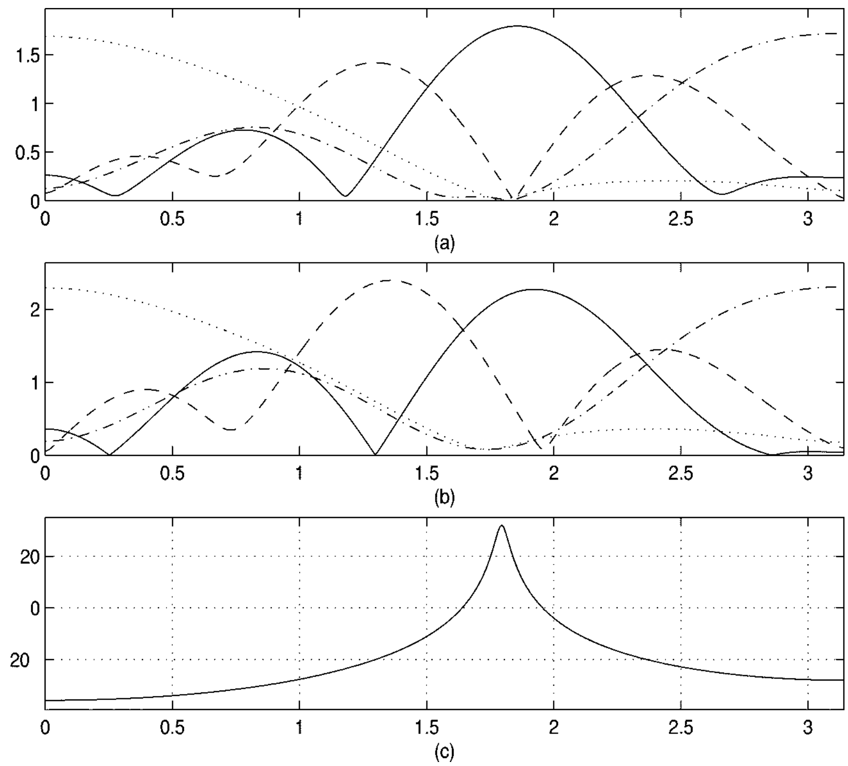

Fig. 7. Example B: (a) Amplitude responses of filters H_0 (solid line), H_1 (dashed line), H_2 (dash-dotted line), and H_3 (dotted line). (b) Amplitude responses of filters F_0 (solid line), F_1 (dashed line), F_2 (dash-dotted line), and F_3 (dotted line). (c) Power spectral density $S_{xx}(e^{j\omega})$ in decibels.

TABLE I
CODING GAIN COMPARISONS FOR EXAMPLES A AND B

θ	Coding Gain				
	DCT	KLT	Brick Wall Filter	Orthonormal	Biorthogonal
$\pi/1.75$	1.3684	3.3473	2.8383	4.2512	4.9174
$\pi/2.8$	1.4127	3.7674	4.4431	5.8555	6.6411

where $\boldsymbol{P}_r^*$ and $\boldsymbol{Q}_r^*$ are the matrices $\boldsymbol{P}_r$ and $\boldsymbol{Q}_r$ evaluated using $\boldsymbol{h}^*$ and $\boldsymbol{f}^*$, respectively. Accordingly, the constraint in (61) becomes

$$\boldsymbol{e}_3^T \Delta \boldsymbol{h} = 0 \tag{71}$$

where

$$\boldsymbol{e}_3 = [1\ 2\ \cdots\ 2]^T \in \mathbb{R}^{((N_1/2)+1)\times 1}.$$

By combining (70) with (71), we find that $\Delta\boldsymbol{h}$ is required to satisfy

$$\boldsymbol{Q}_e \Delta \boldsymbol{h} = \boldsymbol{\gamma}_3 \tag{72}$$

where

$$\boldsymbol{Q}_e = \begin{bmatrix} \boldsymbol{Q}_r^* \\ \boldsymbol{e}_3^T \end{bmatrix}, \qquad \boldsymbol{\gamma}_3 = \begin{bmatrix} -\boldsymbol{P}_r^* \boldsymbol{f}^* + \boldsymbol{e}_r \\ 0 \end{bmatrix}.$$

The linear system in (72) contains $(N_1 + N_2 + 6)/4$ equations and $(N_1 + 2)/2$ unknown components, which leads to the number of degrees of freedom

$$\hat{\eta} = \frac{N_1 - N_2 - 2}{4}. \tag{73}$$

Recall that the filter lengths N_1 and N_2 are assumed to be even with $N_1 > N_2$ and $(N_1 + N_2)/2$ odd. This implies that N_1 is related to N_2 in terms of the equation

$$N_1 = N_2 + 2(2k+1), \qquad \text{for some integer } k \geq 0. \tag{74}$$

Hence

$$\hat{\eta} = k. \tag{75}$$

If $k = 0$, i.e., $N_1 = N_2 + 2$, then (72) is a square and nonsingular system with the unique solution

$$\Delta \boldsymbol{h} = \boldsymbol{Q}_e^{-1} \boldsymbol{\gamma}_3. \tag{76}$$

Since $\boldsymbol{x}^*$ well approximates the PR condition, $\Delta\boldsymbol{h}$ given by (76) is a vector with small magnitude, and the outcome of the second stage of the design is given by

$$\boldsymbol{x}^{**} = \begin{bmatrix} \boldsymbol{h}^* + \Delta\boldsymbol{h} \\ \boldsymbol{f}^* \end{bmatrix}. \tag{77}$$

If $k > 0$, then all the solutions of (72) are characterized by

$$\Delta\boldsymbol{h} = \boldsymbol{\delta}_3 + \boldsymbol{V}_{\hat{\eta}}\boldsymbol{\zeta} \tag{78}$$

where $\boldsymbol{\delta}_3 = \boldsymbol{Q}_e^{\dagger}\gamma_3$, $\boldsymbol{V}_{\hat{\eta}}$ is the matrix formed by using the last $\hat{\eta}$ columns of matrix $\boldsymbol{V}_e$ from the SVD of $\boldsymbol{Q}_e = \boldsymbol{U}_e\boldsymbol{\Sigma}_e\boldsymbol{V}_e$, and $\boldsymbol{\zeta}$ is an $\hat{\eta}$-dimensional parameter vector. The free parameter vector $\boldsymbol{\zeta}$ can be used to further reduce the objective function $\Phi(\boldsymbol{x})$ in (54). Since $\boldsymbol{f}^*$ is now fixed, minimizing $\Phi(\boldsymbol{x}^* + \Delta\boldsymbol{x})$ is equivalent to solving the optimization problem

$$\underset{\boldsymbol{\zeta}}{\text{minimize}} \quad \hat{\Phi}(\boldsymbol{\zeta}) = [(\hat{\boldsymbol{h}}^* + \boldsymbol{V}_{\hat{\eta}}\boldsymbol{\zeta})^T\boldsymbol{R}_n(\hat{\boldsymbol{h}}^* + \boldsymbol{V}_{\hat{\eta}}\boldsymbol{\zeta})] \cdot [(\hat{\boldsymbol{h}}^* + \boldsymbol{V}_{\hat{\eta}}\boldsymbol{\zeta})^T\boldsymbol{Q}_n(\hat{\boldsymbol{h}}^* + \boldsymbol{V}_{\hat{\eta}}\boldsymbol{\zeta})]. \tag{79}$$

For applications in image compression, typical values of $\hat{\eta}$ are in the range $0 \le \hat{\eta} \le 2$; hence (79) is an unconstrained optimization problem that involves only one or two variables. If we denote a local minimizer of (79) as $\boldsymbol{\zeta}^*$, then the solution of the design problem is given by

$$\boldsymbol{x}^{**} = \begin{bmatrix} \boldsymbol{h}^* + \boldsymbol{\delta}_3 + \boldsymbol{V}_{\hat{\eta}}\boldsymbol{\zeta}^* \\ \boldsymbol{f}^* \end{bmatrix}. \tag{80}$$

V. Design Examples

We now present four examples to illustrate the design methods described in Sections III and IV. In the first two examples, we designed four-channel biorthogonal filter banks with filter length $N = 8$. The input signal was an autoregressive process AR(2) with poles at $0.975e^{\pm j\theta}$ where the values of θ are specified below. We applied the algorithm proposed in Section III with an initial point that corresponds to an orthonormal four-channel filter bank designed using the method proposed in [10] and [23].

Example A: With $\theta = \pi/2.8$ and $\varepsilon = 6 \times 10^{-7}$ in the AR(2) process, it took the algorithm 39 iterations to converge to the solution $\boldsymbol{x} = \boldsymbol{x}^*$. The frequency responses of the various filters and power spectral density are shown in Fig. 6. The objective function $\Phi(\boldsymbol{x})$ was reduced from the original value of $\Phi(\boldsymbol{x}_0) = 1.2979 \times 10^{-8}$ to $\Phi(\boldsymbol{x}^*) = 7.8443 \times 10^{-9}$ which corresponds to an improvement in the coding gain from 5.8555 to 6.6411. The PR constraint was satisfied to within the Frobenius norm (F-norm) value

$$\|\boldsymbol{P}_0^T\boldsymbol{Q}_0\|_F + \|\tfrac{1}{4}\boldsymbol{J} - \boldsymbol{P}_0^T\boldsymbol{Q}_1 - \boldsymbol{P}_1^T\boldsymbol{Q}_0\|_F + \|\boldsymbol{P}_1^T\boldsymbol{Q}_1\|_F = 2.3405 \times 10^{-9}. \tag{81}$$

Example B: With $\theta = \pi/1.75$, $\varepsilon = 2 \times 10^{-7}$, and an initial point that corresponds to an orthonormal filter bank, it took the algorithm 37 iterations to converge to the solution $\boldsymbol{x} = \boldsymbol{x}^*$. The results obtained are plotted in Fig. 7. The objective function was reduced from $\Phi(\boldsymbol{x}_0) = 4.6717 \times 10^{-8}$ to $\Phi(\boldsymbol{x}^*) = 2.6096 \times 10^{-8}$. In this case, the coding gain was increased from 4.2512 to 4.9174. The F-norm in (81) was 6.3876×10^{-10}.

The coding gains of the biorthogonal filter banks designed are compared with those of the discrete-cosine transform (DCT) based, Karhunen–Loéve transform (KLT) based, brick-wall-filter based, and the orthonormal four-channel filter banks in Table I. From the table it is observed that the optimal biorthogonal filter banks designed offer improved coding gains over several orthogonal transform coders as well as the optimal orthonormal subband coder.

TABLE II
Filter Coefficients for Examples C and D

Example C		Example D	
h_0^*	f_0^*	h_0^*	f_0^*
0.1199336126	−0.0352836130	0.0793347557	−0.3502983702
0.1485891876	−0.0437138787	−0.0449592738	−0.1985152686
−0.1394533112	0.5003663650	0.0290358572	0.8555481808
0.4519362058	0.7020461316	0.1993215310	1.4375905277
0.7478924906	0.5003663650	0.4444738905	0.8555481808
0.4519362058	−0.0437138787	0.1993215310	−0.1985152686
−0.1394533112	−0.0352836130	0.0290358572	−0.3502983702
0.1485891876		−0.0449592738	
0.1199336126		0.0793347557	

Example C: Next we applied the method proposed in Section IV to design a two-channel biorthogonal filter bank with $N_1 = 8$ and $N_2 = 6$. The initial point used corresponds to the well-known 9/7 filters (see [24, p. 216]) with

$$\begin{aligned} \boldsymbol{h}_0 &= [\,1 \quad 0 \quad -8 \quad 16 \quad 46 \quad 16 \quad -8 \quad 0 \quad 1\,]^T/64 \\ \boldsymbol{f}_0 &= [-1 \quad 0 \quad 9 \quad 16 \quad 9 \quad 0 \quad -1\,]^T/16. \end{aligned}$$

Again we used an AR(2) process with $\theta = \pi/1.5$ as the input signal. With $\varepsilon = 10^{-6}$ it took the algorithm 25 iterations to converge to a solution $\boldsymbol{x}^*$ which reduced the objective function from $\Phi(\boldsymbol{x}_0) = 1.0622$ to $\Phi(\boldsymbol{x}^*) = 0.0932$; this corresponds to a coding gain increase from 0.9703 to 3.2753. The point $\boldsymbol{x}^*$ satisfies the PR condition approximately with

$$\|-\boldsymbol{P}_r^*\boldsymbol{f}^* + \boldsymbol{e}_r\| = 0.6377 \times 10^{-9}. \tag{82}$$

The second stage of the design resulted in the solution in columns 1 and 2 of Table II, for which the 2-norm in (82) is further reduced to 0.4178×10^{-16}. The coding gain associated with $\boldsymbol{x}^{**}$ was approximately the same as that for $\boldsymbol{x}^*$, i.e., 3.2753. The amplitude responses of the filters and the power spectral density corresponding to $\boldsymbol{x}^{**}$ are shown in Fig. 8.

Example D: Next we considered an AR(2) process with $\theta = \pi/1.25$ as the input signal. With the same initial point and ε, the two-stage design resulted in the solution shown in columns 3 and 4 of Table II, which reduced the objective function from $\Phi(\boldsymbol{x}_0) = 0.2153$ to $\Phi(\boldsymbol{x}^{**}) = 0.0534$; this corresponds to a coding gain improvement from 2.1554 to 4.3267. The results obtained are plotted in Fig. 9.

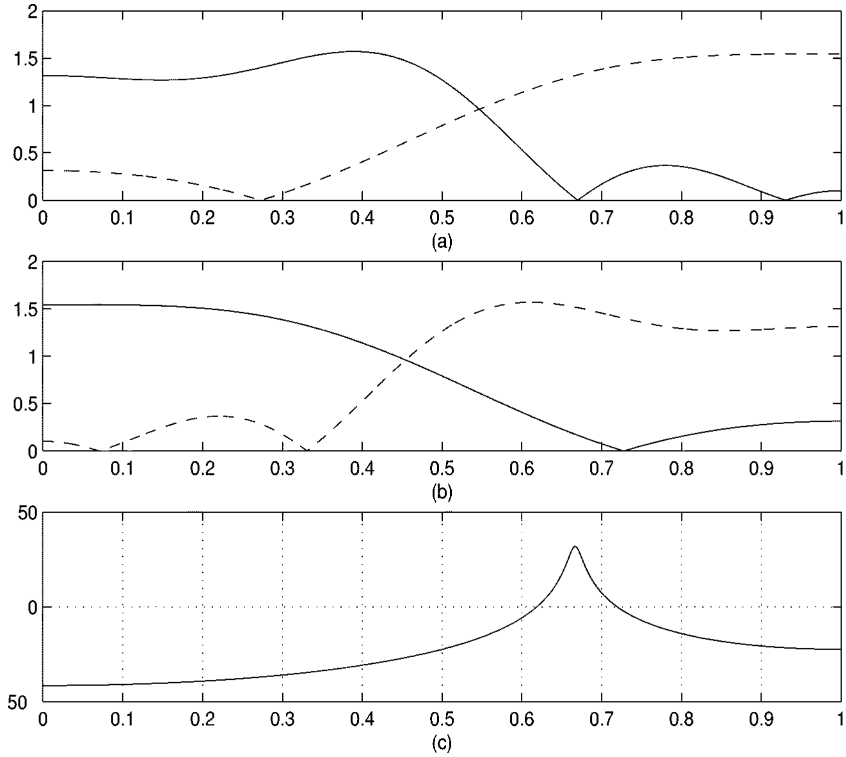

Fig. 8. Example C: (a) Amplitude responses of filters H_0 (solid line) and H_1 (dashed line). (b) Amplitude responses of filters F_0 (solid line) and F_1 (dashed line). (c) Power spectrum density $S_{xx}(e^{j\omega})$ in decibels.

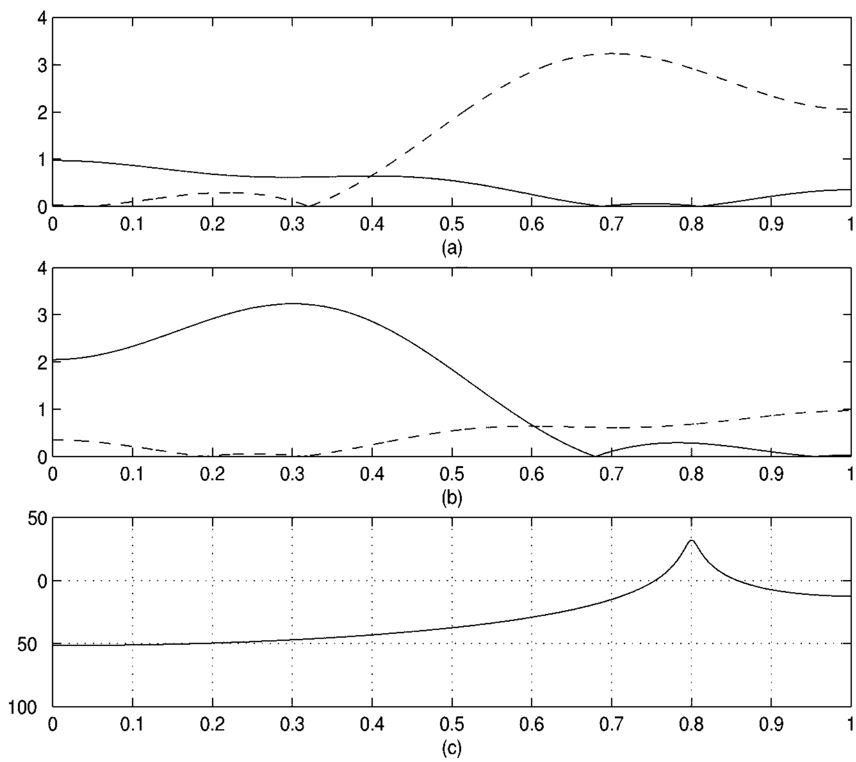

Fig. 9. Example D: (a) Amplitude responses of filters H_0 (solid line) and H_1 (dashed line). (b) Amplitude responses of filters F_0 (solid line) and F_1 (dashed line). (c) Power spectrum density $S_{xx}(e^{j\omega})$ in decibels.

VI. Conclusion

We have proposed an optimization based approach for the design of M-channel biorthogonal filter banks that are adapted to the statistics of the input signal. By parameterizing a first-order approximation of the PR constraint, we were able to convert the constrained nonlinear minimization problem of size $2MN$ to an iterative line-search problem. The solution obtained satisfies the

PR condition only approximately but an arbitrary precision can be achieved in practice by reducing the termination tolerance of the algorithm. We have also shown for the two-channel case that if the analysis and synthesis lowpass filter lengths are different, a refinement of the algorithm is possible that leads to a solution in a very small neighborhood of a local minimizer, which satisfies the PR constraint precisely.

Like many nonlinear optimization algorithms, the proposed design algorithms do not guarantee a global minimizer. For a local minimizer to be satisfactory, it is of critical importance to start the minimization with a good initial point. This simply means that one should, as far as possible, start with any known good suboptimal design.

REFERENCES

[1] A. N. Akansu and Y. Liu, "On signal decomposition techniques," *Opt. Eng.*, vol. 30, pp. 912–920, July 1991.

[2] J. Katto and Y. Yasuda, "Performance evaluation of subband coding and optimization of its filter coefficients," in *Proc. SPIE Visual Commun. Image Processing*, Nov. 1991, pp. 95–106.

[3] P. Delsarte, B. Marq, and D. Slock, "Signal-adapted multiresolution transform for image coding," *IEEE Trans. Inform. Theory*, vol. 38, pp. 897–904, Mar. 1992.

[4] M. Unser, "On the optimality of ideal filters for pyramid and wavelet signal approximation," *IEEE Trans. Signal Processing*, vol. 41, pp. 3591–3596, Dec. 1993.

[5] M. K. Tsatsanis and G. B. Giannakis, "Principal component filter banks for optimal multiresolution analysis," *IEEE Trans. Signal Processing*, vol. 43, pp. 1766–1777, Aug. 1995.

[6] P. Moulin, "A new look at signal-adapted QMF bank design," in *Proc. Int. Conf. Acoust., Speech, Signal Processing*, Detroit, MI, May 1995, pp. 1312–1315.

[7] I. Djokovic and P. P. Vaidyanathan, "On optimal analysis/synthesis filters for coding gain optimization," *IEEE Trans. Signal Processing*, vol. 44, pp. 1276–1279, May 1996.

[8] P. P. Vaidyanathan, "Theory of optimal orthonormal filter banks," in *Proc. Int. Conf. ASSP*, Atlanta, May 1996.

[9] K. C. Aas and C. T. Mullis, "Minimum mean-squared error transform coding and subband coding," *IEEE Trans. Inform. Theory*, vol. 42, pp. 1179–1192, July 1996.

[10] P. Moulin and M. K. Mihçak, "Theory and design of signal-adapted FIR paraunitary filter banks," *IEEE Trans. Signal Processing*, vol. 46, pp. 920–929, April 1998.

[11] P. P. Vaidyanathan and A. Kiraç, "Results on optimal biorthogonal filter banks," *IEEE Trans. Circuits Syst., II*, vol. 45, pp. 932–947, Aug. 1998.

[12] M. Antonini, M. Barland, P. Mathieu, and I. Daubechies, "Image coding using wavelet transform," *IEEE Trans. Image Processing*, vol. 1, pp. 205–220, Apr. 1992.

[13] S. O. Aase and T. Ramstad, "On the optimality of nonunitary filter banks in subband coders," *IEEE Trans. Image Processing*, vol. 4, pp. 1585–1591, Dec. 1995.

[14] A. Papoulis, *Probability, Random Variables, and Stochastic Processes*. New York: McGraw-Hill, 1991.

[15] P. P. Vaidyanathan, *Multirate Systems and Filter Banks*. Englewood Cliffs, NJ: Prentice-Hall, 1993.

[16] K. Nayebi, T. P. Barnwell III, and M. J. T. Smith, "Time-domain filter bank analysis: A new design theory," *IEEE Trans. Signal Processing*, vol. 40, pp. 1412–1429, June 1992.

[17] T. D. Tran and T. Q. Nguyen, "On M-channel linear phase FIR filter banks and application in image compression," *IEEE Trans. Signal Processing*, vol. 45, pp. 2175–2187, Sept. 1997.

[18] R. A. Horn and C. R. Johnson, *Matrix Analysis*. Cambridge, U.K.: Cambridge Univ. Press, 1985.

[19] R. Fletcher, *Practical Methods of Optimization*, 2nd ed. New York: Wiley, 1987.

[20] J. Shapiro, "Embedded image coding using zerotrees of wavelet coefficients," *IEEE Trans. Acoust., Speech Signal Processing*, vol. 41, pp. 3445–3462, Dec. 1993.

[21] J. D. Villasenor, B. Belzer, and J. Liao, "Wavelet filter evaluation for image compression," *IEEE Trans. Image Processing*, vol. 4, pp. 1053–1060, Aug. 1995.

[22] A. Said and W. A. Pearlman, "A new, fast, and efficient image codec based on set partitioning in hierarchical tree," *IEEE Trans. Circuits Syst. Video Technol.*, vol. 6, pp. 243–250, June 1996.

[23] A. Kiraç and P. P. Vaidyanathan, "Theory and design of optimum FIR compaction filters," *IEEE Trans. Signal Processing*, vol. 46, pp. 903–919, Apr. 1998.

[24] G. Strang and T. Nguyen, *Wavelets and Filter Banks*. Cambridge, MA: Wellesley-Cambridge, 1996.

Wu-Sheng Lu (S'81–M'85–SM'90–F'99) received the B.S. degree in mathematics from Fudan University, China, in 1964, and the M.S. degree in electrical engineering and the Ph.D. degree in control science from the University of Minnesota, Minneapolis, MN, in 1983 and 1984, respectively.

He was a Postdoctoral Fellow at the University of Victoria, BC, Canada, in 1985 and Visiting Assistant Professor at the University of Minnesota in 1986. Since 1987, he has been with the University of Victoria where he is currently Professor. His teaching and research interests are in the areas of digital signal processing and numerical optimization. He is the coauthor with A. Antoniou of *Two-Dimensional Digital Filters* (New York: Marcel Dekker, 1992). He was Associate Editor for the Canadian Journal of Electrical and Computer Engineering in 1989 and the Editor of the same journal from 1990 to 1992.

Dr. Lu is a Fellow of the Engineering Institute of Canada. He was elected Fellow of the IEEE for contributions to multidimensional and multirate digital filters and discrete systems. He was an Associate Editor of IEEE TRANSACTIONS ON CIRCUITS AND SYSTEMS II from 1993 to 1995. Presently he serves as an Associate Editor for the IEEE TRANSACTIONS ON CIRCUITS AND SYSTEMS I and for the *International Journal of Multidimensional Systems and Signal*.

Andreas Antoniou (M'69–SM'79–F'82) received the B.Sc. (Eng.) and Ph.D. degees in electrical engineering from the University of London, U.K., in 1963 and 1996, respectively.

From 1966 to 1969, he was Senior Scientific Officer at the Post Office Research Department, London, U.K., and from 1969 to 1970, he was a member of the Scientific Staff at the R & D Laboratories of Northern Electric Company Ltd., Ottawa, ON, Canada. From 1970 to 1983, he served in the Department of Electrical and Computer Engineering, Concordia University, Montreal, Canada, as Professor from June 1973 and as Chairman from December 1977. He served as founding Chairman of the Department of Electrical and Computer Engineering, University of Victoria, Victoria, BC, Canada, from July 1, 1983 to June 30, 1990 and is now Professor in the same department. His teaching and research interests are in the areas of electronics, network synthesis, digital system design, active and digital filters, and digital signal processing. He published extensively in these areas. One of his papers on gyrator circuits was awarded the Ambrose Fleming Premium by the Institution of Electrical Engineers, U.K. He is the author of *Digital Filters: Analysis, Design, and Applications* (New York: McGraw-Hill) and the coauthor with W.-S. Lu of *Two-Dimensional Digital Filters* (New York: Marcel Dekker, 1992).

Dr. Antoniou is a member of the Association of Professional Engineers and Geoscientists of British Columbia, and Fellow of the Institution of Electrical Engineers. He was elected Fellow of the Institute of Electrical and Electronic Engineers for contributions to active and digital filters, and to electrical engineering education. He served as Associate Editor of IEEE TRANSACTIONS ON CIRCUITS AND SYSTEMS from June 1983 to May 1985 and as Editor from June 1985 to May 1987, and was a member of the Board of Governors of the Circuits and Systems Society during 1995–1997. He was recently awarded a CAS Golden Jubilee Medal by the IEEE Circuits and Systems Society in recognition of outstanding achievements in the area of circuits and systems and the British Columbia Science Council Chairman's Award for Career Achievement.